

## Article

# Mineralogical Characterization of Raw Clay from Rujište (Serbia) Used in Traditional Pottery Manufacture

Maja Milošević <sup>1,\*</sup>, Predrag Dabić <sup>1</sup>, Jelena Gulicovski <sup>2</sup>, Vladimir Dodevski <sup>2</sup> and Milena Rosić <sup>2,\*</sup>

<sup>1</sup> Faculty of Mining and Geology, University of Belgrade, Đušina 7, 11000 Belgrade, Serbia; predrag.dabic@rgf.bg.ac.rs

<sup>2</sup> “Vinča” Institute of Nuclear Sciences, National Institute of the Republic of Serbia, University of Belgrade, Mike Petrovića Alasa 12–14, 11351 Belgrade, Serbia; rocenj@vin.bg.ac.rs (J.G.); vladimir@vin.bg.ac.rs (V.D.)

\* Correspondence: maja.milosevic@rgf.bg.ac.rs (M.M.); mrosic@vin.bg.ac.rs (M.R.)

**Abstract:** The pottery produced from the Rujište deposit in Serbia has been protected under the guidance of UNESCO and the Sector for Intangible Cultural Heritage of Serbia since 2019. A study was conducted to evaluate the mineralogical characteristics of the raw clay from this deposit. This study used various techniques, such as X-ray diffraction (XRD), infrared (IR) spectroscopy, X-ray fluorescence (XRF), and differential thermal analysis (DTA) to characterize the clay. This study found that the clay contained mostly clay minerals (56.3%–41.9%), with illite, smectite, and chlorite as the predominant phases. Other phases identified were quartz, feldspars, carbonates, and iron-bearing minerals (43.8%–58.1%). The chemical analyses revealed a high abundance of silica (>52 wt.%) and alumina (~16 wt.%), with Fe<sub>2</sub>O<sub>3</sub> (~6 wt.%), K<sub>2</sub>O (~2.8 wt.%), and a similar content of MgO as the main constituents. The physical features that were investigated included the granulometry (clay: ~31%–44%, silt: ~26%–23%, and sand: ~42%–32%), specific surface area (97 to 107 m<sup>2</sup> g<sup>-1</sup>), cation exchange capacity (12.5–13.7 mmol 100 g<sup>-1</sup>), and color (yellowish to moderate brown). The preliminary results suggest that most of the raw clay from the Rujište deposit might be suitable for use in traditional pottery manufacture.

**Keywords:** clay; raw material; pottery; Ražanj



**Citation:** Milošević, M.; Dabić, P.; Gulicovski, J.; Dodevski, V.; Rosić, M. Mineralogical Characterization of Raw Clay from Rujište (Serbia) Used in Traditional Pottery Manufacture. *Minerals* **2024**, *14*, 469. <https://doi.org/10.3390/min14050469>

Academic Editor: Fernando Rocha

Received: 19 March 2024

Revised: 24 April 2024

Accepted: 26 April 2024

Published: 28 April 2024



**Copyright:** © 2024 by the authors. Licensee MDPI, Basel, Switzerland. This article is an open access article distributed under the terms and conditions of the Creative Commons Attribution (CC BY) license (<https://creativecommons.org/licenses/by/4.0/>).

## 1. Introduction

Raw clay materials are considered some of the most important parts of the fabrication of ceramic [1–7] and different types of cosmetic, pharmaceutical, medical, and environmental products [8–15]. Clays also have an important part in several industries and they are applied in the manufacture of paper, paints, pneumatics, building, and other materials [9,16–20]. The manufacture of ceramics, pottery, structural bricks, or tiles involves the application of raw clays with minimal additional processing, directly mined out from the ground in the vicinity of the processing plant. These raw clays, in their untreated form, are easily workable because they already contain different amounts of natural fillers and fluxes alongside the clay minerals (kaolinite, montmorillonite, illite, vermiculite, etc.) in their composition, which makes them more plastic or non-plastic (micas, quartz, feldspars, iron oxides, and hydroxides, like magnetite, hematite, etc.) [20,21]. The traditional technology for manufacturing ceramic materials, including single- and double-firing processes, usually uses clay bodies comprising one type of clay together with non-plastic materials [21,22]. Most clay bodies used for industrial applications are the following three types: marly clays (illite–chlorite clay with smectite and carbonates), red shale (illite + chlorite ± kaolinite ± smectite, and absence of carbonates) and kaolinite–illite ball clay (+ quartz + carbonates or + quartz + feldspars) [16,21]. Minerals, such as carbonates, quartz, feldspar, pyrite, iron oxy/hydroxy minerals, etc., represent the most common impurities that can be present in the raw clay and can affect the main characteristics and utilization of this type of material [22,23]. Raw clays show a unique composition

based on their deposits, which is reflected in their complex mineralogical, chemical, and physical characteristics [3,23–25], among others. It is possible to assess their potential application based on these characteristics; therefore, they must be detailedly investigated. The discovery of the unique properties that various types of clay acquire after being fired led to the development of the synthetic material known as ceramic. The production of ceramic material, in its broad sense, is one of the oldest human activities in history [26,27]. Potters typically do not use raw clay straight from the ground to make ceramics; instead, they process and manipulate it in various ways to create a clay paste or body that is suitable for the specific pottery vessel or ceramic object they want to produce [28–31]. Potters mix dry and moist clay in different proportions and use various methods to blend them into a single paste, resulting in different appearances for the intentionally mixed pastes. They also temper and mix different clay sources to improve the clay's physical behavior during the production, drying, firing, and overall life cycle of the ceramic object. This includes determining the best manufacturing and forming methods for the applied clay, managing shrinkage during drying and firing, and ensuring the strength, toughness, thermal shock resistance, and thermal conductivity of the finished object when in use [29–32].

There are clay deposits in Serbia that mostly contain abundant amounts of illite–mica clay, along with varying amounts of kaolinite or smectite-type clays (and/or I/S mixed layers). These deposits also have secondary minerals, such as quartz, feldspar, carbonates, chlorites, and hematite [33–35]. There are several significant locations in the municipality of Ražanj that date back to the time of the first settled communities engaged in agriculture and animal husbandry about 7000 years ago [36]. The oldest and most well-explored evidence of artefacts belonging to the Vinča culture and the Bronze and Iron Ages can be found at Crnokalačka bara, located on the border between the villages of Rujište and Crni Kao [36]. In the Ražanj municipality of Serbia, the Rujište deposit has raw clay that is traditionally used for pottery making and cosmetic purposes. This area has enabled the production of a specific type of hand-made unglazed pottery, earthenware called “crepulja”, a shallow circular bread-baking pan. It received its name because it is manufactured using a similar method as roofing tiles. We found the first mention of the production of crepulja in Ražanj in 1928, made by Savić [37]. The most extensive research into the production of Ražanj “crepulja” pans was performed years later by Petrović in 1936 [36]. In his work, he described in detail the location and appearance of the raw materials used for making the characteristic pottery, tools, and methods of preparing the clay, shaping, and firing, with reference to their sale and distribution but without any geological or mineralogical data about the samples [36]. Production of this pottery continued through the years, and in 2019, it became protected under the guidance of the Sector for Intangible Cultural Heritage of Serbia, which includes elements determined by UNESCO [35]. Making pottery in the village of Rujište near Ražanj is a craft that has been passed down since the 19th century. The specific variety of pottery, crepulja, is made using two types of raw clay material and one type of sand sourced from the same location, called “Crepuljarsko brdo”, in the village of Rujište, part of the municipality of Ražanj. The process of making pottery includes digging the necessary clay, mixing it by trampling, shaping it by hand, drying it, “tinning” it with scraps of tiles, spraying it with water, and smoothing it. The pottery is then allowed to dry and is smoked before being baked in a “furuna” (a wood-fired furnace) [35]. After firing, the pottery is tied with wire and then covered in the ash from the furnace while no other glazes are added. The pottery comes in three different sizes and can have a hole in the middle, although there are also versions without the hole that are used for cooking rather than baking. In the village of Rujište, men traditionally produce this type of pottery, but today, women are also starting to take up this craft.

This paper aims to provide an overview of the mineralogical and chemical properties of the raw clay from Rujište traditionally applied in pottery production, which has been protected since 2019 under the guidance of the Sector for Intangible Cultural Heritage of Serbia, as determined by UNESCO. Unfortunately, there are no detailed descriptions of the composition of clays in this area, although several ethnographic and archaeological

studies have been conducted on the pottery [36]. Data about the applied raw clay materials are still scarcely available. Therefore, this type of investigation is the first of its kind for the mentioned raw clay material. The information obtained will be used to gain a better understanding of its main characteristics and will consequently provide a useful means for future identification of the provenance for archaeological ceramics in this region.

## 2. Geological and Geographical Setting

The Rujiste deposit can be found in the municipality of Ražanj, which is situated in the southeast part of Serbia, about 185 km away from Belgrade, the capital of the country. Raw clay from two localities in the Ražanj area has been investigated and found to be mostly Neogene sediments (Figure 1). According to the geological map, this locality is extensive and rich in sediments, consisting mainly of microcrystalline carbonate minerals mixed with clay minerals and a small amount of detrital quartz and feldspar. The geological map of the area reveals that the Middle Miocene is transgressive over the Jurassic and Lower Cretaceous limestones, and it includes conglomerates, freshwater limestones, and different colored types of clays (red, green, and grey) [38,39]. The location marked with a star on the map represents the source of the two samples that were collected for the investigations. This area has two types of sediment from different stratigraphic units. The first is conglomeratic sandstone, while the second is marly–clayey sediment. These layers lie discordantly over the basic highlands and rise under the marly–clayey sediments. In the lower parts of the series, there are widespread conglomerates, sandstones, agglomerates with intercalations of red and green clays, and argillaceous sandstones. In the higher parts of the unit, there are finer sediments, including marls, sandstones, and marls with tuffs and tuffites [38,39]. These sediments pass into fine-grained conglomerates of chlorite and sericite schists, quartzite, limestone, and andesite. Conglomerates are replaced by subarkoses and layers of coarsely dispersed clays. The detrital component of these sediments consists of quartz, feldspar, chlorite, sericite schists, quartzite, and limestone which is also cemented with a clay–carbonate material [38,39].

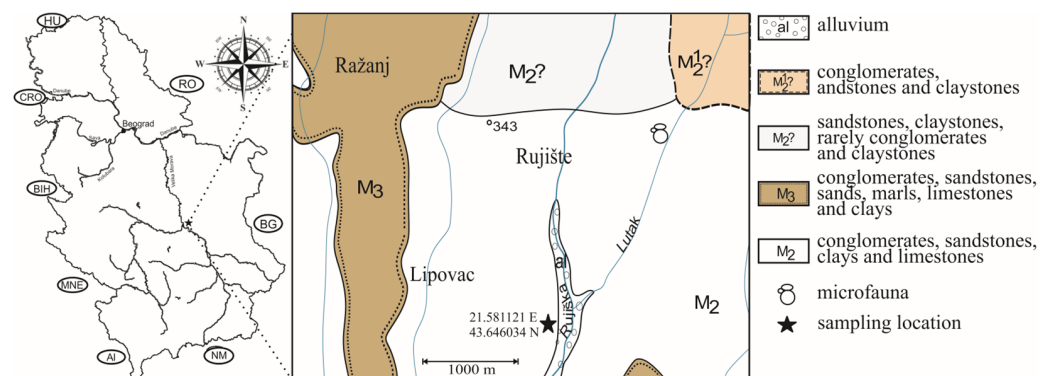


**Figure 1.** Geological and geographical setting and location of the investigated samples.

## 3. Materials and Methods

The area under investigation consists of two distinct clay layers that are separated by color. The first layer is located in the upper parts of the deposit and is made up of light brown clay (sample 1) while the second layer, located in the lower parts of the deposit, comprises dark brown-colored clay (sample 2) (Figure 2). Not only was the color considered when choosing these samples but also the pottery manufacturer's recommendation as these raw clays represent materials that they use for production. The two collected samples, around 1 kg each, were firstly dried at room temperature, then crushed and homogenized.



**Figure 2.** Investigated samples from Rujiste deposit: 1-light brown clay (sample 1), 2-dark brown-colored clay (sample 2).

Powder XRD data were obtained on a Rigaku SmartLab powder X-ray diffractometer (40 kV, 30 mA) at room temperature using Bragg–Brentano geometry and  $\text{CuK}\alpha$  radiation. The measurements were performed on bulk samples, as well as on clay fractions below  $2\ \mu\text{m}$ , separated by gravitational settling. Oriented aggregates were made from the fraction  $< 2\ \mu\text{m}$  using the glass slide method. The oriented samples were examined as air-dried (AD), after solvation with ethylene glycol (EG), and after heating at  $550\ ^\circ\text{C}$  for 1 h (H). The scan range was from  $2$  to  $70^\circ\ 2\theta$  (for bulk samples and clay fractions) and from  $2$  to  $30^\circ\ 2\theta$  (for oriented aggregates) with a scanning speed of  $5^\circ/\text{min}$  and a step size of  $0.01$ . PDXL 2 integrated X-ray powder diffraction software [40] with the PDF-2 database [41] was used for mineral phase identification and semi-quantitative phase analysis using the whole-powder-pattern fitting (WPPF) method incorporated in this software. Whole-rock major ( $\text{SiO}_2$ ,  $\text{Al}_2\text{O}_3$ ,  $\text{Fe}_2\text{O}_3(\text{t})$ ,  $\text{MnO}$ ,  $\text{MgO}$ ,  $\text{CaO}$ ,  $\text{Na}_2\text{O}$ ,  $\text{K}_2\text{O}$ ,  $\text{TiO}_2$ ,  $\text{P}_2\text{O}_5$ ,  $\text{SO}_3$ ,  $\text{Cr}_2\text{O}_3$ , and  $\text{NiO}$ ) and trace (Ba, Ce, Co, Cr, Cs, Cu, Ga, La, Nb, Nd, Ni, Pb, Pr, Rb, Sc, Sm, Sr, Th, U, V, W, Y, Zn, and Zr) elements were measured on 10g fused discs and powder press tablets, respectively. The measurements were performed routinely on a Philips MagiX Pro at the Institute of Geosciences at the University of Mainz. Infrared spectroscopic (IR) analysis was performed by application of the Perkin Elmer 597 spectrometer and the standard KBr pellet method in the region of  $4000\text{--}200\ \text{cm}^{-1}$ . Differential thermal analysis (DTA) was performed over a temperature range of  $20\text{--}1100\ ^\circ\text{C}$  and a heating rate of  $10\ ^\circ\text{C}/\text{min}$  by application of the Adamel furnace equipped with a Pt–PtRh thermocouple and a power controller by Powersupply. All measurements were performed in an air atmosphere using  $\text{Al}_2\text{O}_3$  as the reference material. The grain-size distribution was determined using the pipette method according to the DIN ISO 11,277 (2002) after sieving for fractions higher than silt. The cation exchange capacity (CEC) alongside the specific surface area (SSA) of the samples was determined after saturation with methylene blue (MB) solution according to the corresponding standard [42] followed by uniSPEC2 spectrophotometer. The colors of the raw powder samples were visually compared with Munsell color cards.

#### 4. Results and Discussion

An X-ray powder diagram of samples 1 and 2 is given in Figure 3. A database search revealed that the sample contains minerals: quartz (ICDD # 01-085-1054), illite/mica (ICDD # 00-058-2034), chlorite group mineral (ICDD # 01-074-1137), plagioclase group mineral (ICDD # 01-080-1094), smectite and/or interstratified illite/smectite (ICDD # 00-060-0318), and calcite (ICDD # 01-083-4601). A small amount of K-feldspar and dolomite is also possible.

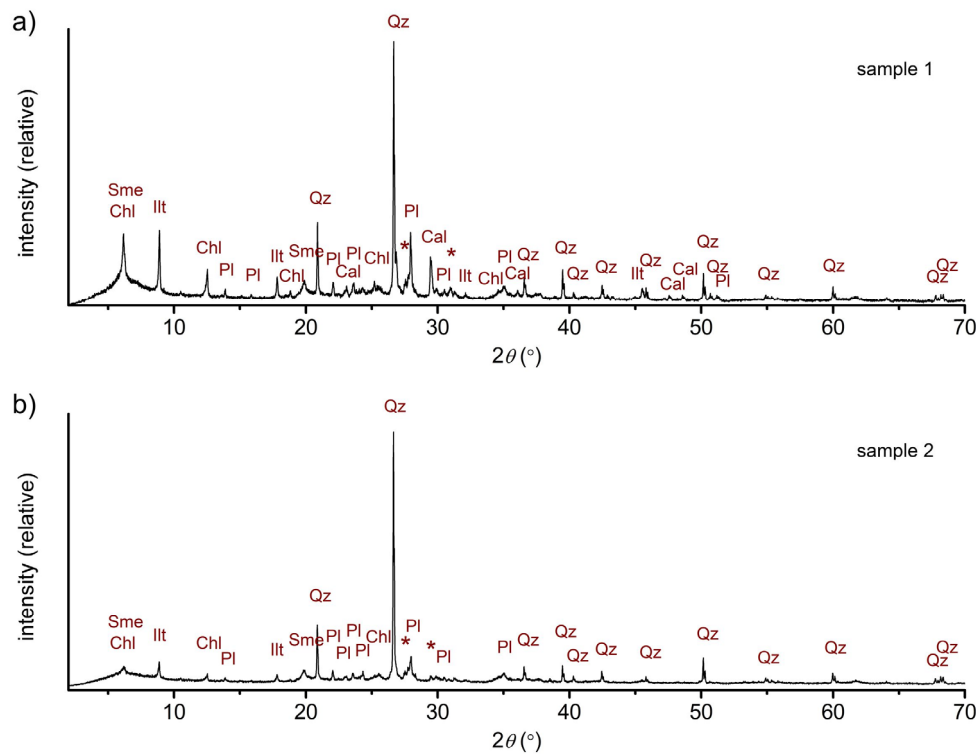


**Figure 3.** X-ray powder diffractograms of: (a) sample 1 and (b) sample 2. Legend: Qz—quartz; Illt—illite/mica; Sme—smectite; Chl—chlorite; Pl—plagioclase; Cal—calcite; \*—denotes diffraction peaks originating from possible present phases.

A database search revealed that the following minerals were present in the sample: quartz, illite/mica, chlorite group mineral, plagioclase group mineral, and a mineral from the smectite group. It is also possible that a small amount of K-feldspar and calcite was present. Figure 4 shows the powder diffractogram of the investigated samples tested on clay fractions below 2 μm, separated by gravitational settling.

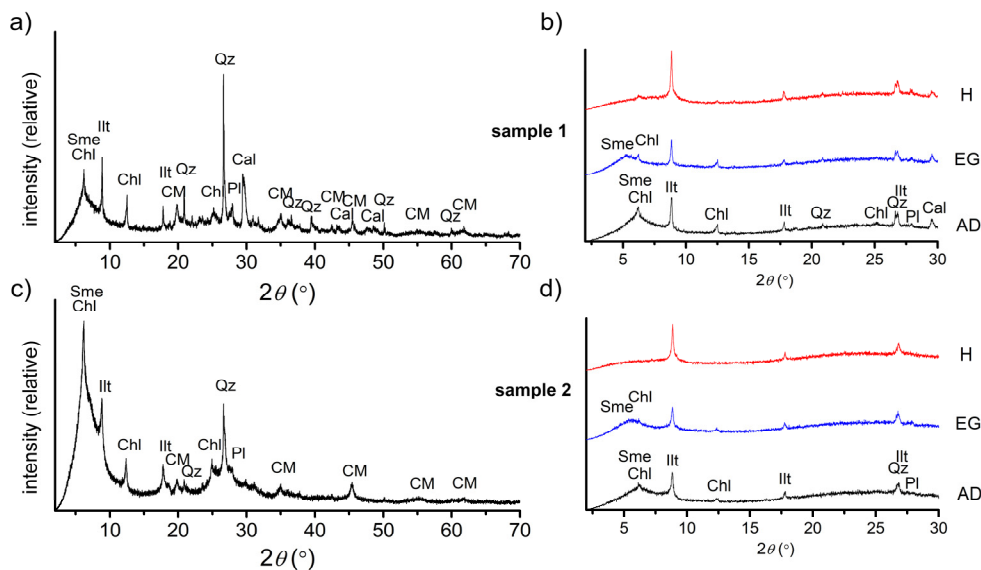


**Figure 4.** Diffractograms of clay fraction (<2 μm): powder (a) and oriented (b) aggregates of sample 1; powder (c) and oriented (d) aggregates of sample 2. Legend: Illt—illite; Sme—smectite; Chl—chlorite; Qz—quartz; Pl—plagioclase; Cal—calcite; CM—indicates clay minerals’ joint diffraction peaks; AD—air-dried; EG—saturated with ethylene glycol; H—heated.

The results of the quantitative phase analysis (Table 1) show a higher amount of quartz in sample 2 than the sample 1. A smaller amount of chlorite was present in sample 2 compared to sample 1, while other identified mineral phases were present in similar amounts in both samples.

**Table 1.** Results of the quantitative phase analysis (%).

	Illite	Smectite	Chlorite	Quartz	Plagioclase	Calcite
Sample 1	30.1	6.3	19.9	24.8	12.1	6.9
Sample 2	28.6	4.7	8.6	42.9	15.2	-

According to Abadir [43] and Jackson [44], the presence of quartz is necessary in the clay body for the manufacture of all types of traditional ceramics to decrease the shrinkage of the manufactured object, although it also reduces the body’s tendency to distort when fired. The feldspar group of minerals, along with illite, mica, and chlorites, are considered “flux-saturated” minerals that provide the clay body with K<sub>2</sub>O, Na<sub>2</sub>O, Al<sub>2</sub>O<sub>3</sub>, and SiO<sub>2</sub> and affect the glaze melt. While they are favorable as flux agents, higher amounts of these minerals make poor bases for functional pottery and can contribute to a high surface tension; thus, they do not suspend well, leading to settling in a hard layer and drying into a powdery surface [1,43,44]. Since pottery in the Ražanj municipality has been in production for a long time, it is evident that the contents of flux minerals in the clay minerals and their interaction in the clay body are at the necessary proportions for successful production.

The particle size distribution of clay is crucial for determining the properties of suspensions, such as plasticity and viscosity, and the effects that occur during drying and firing [45]. Samples 1 and 2 contained 31.2% and 44.5% clay, 26.4% and 23.4% silt, and 42.3% and 32.2% sand, respectively. The results are represented graphically (Figure 5) in a ternary diagram to show the proportions of clay, silt, and sand fractions in our samples [46,47].

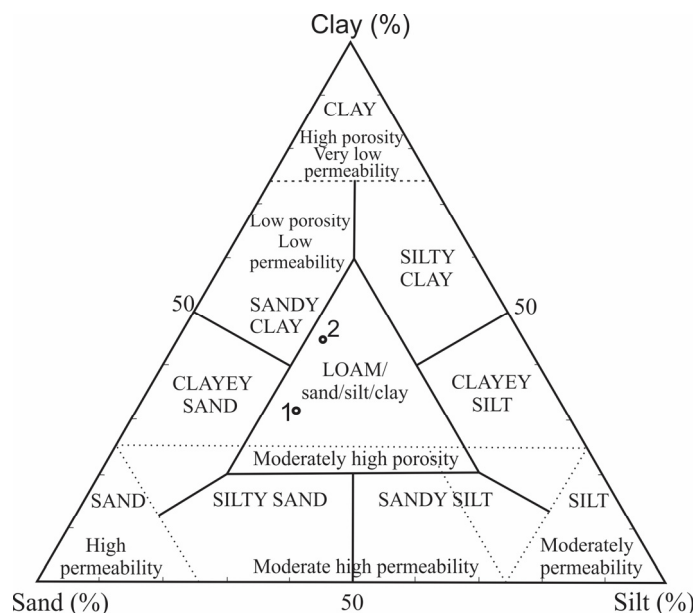


**Figure 5.** A ternary diagram of the investigated samples showing the particle size distribution (adapted from [6,46,47]).

Both samples can be described, according to the diagram, as loam, with roughly equal proportions of sand, silt, and clay, and moderately high porosity. Sample 1 had more of a clayey–sand granulation, while sample 2 had a higher clay fraction. The high percentage of quartz, observed by XRD analysis, was corroborated by the high percentage of sand and silt in both samples. As previously mentioned, both samples had moderately high porosity,

which is preferable since high permeability leads to low cohesion and implies difficulties for extrusion processes [6,48].

The DTA data obtained for samples 1 and 2 are represented in Figure 6. Endothermic reactions in the temperature range of 100–200 °C are caused by the loss of moisture and interlayer water present in the phyllosilicate structure [49]. Among the reactions attributed to the interlayer water, there are also peaks corresponding to the presence of minerals from the mica and chlorite groups. An endothermic reaction around 200 °C usually indicates the presence of smectites, such as montmorillonite or illite [50]. A band around 180 °C is observed for sample 1, indicating a higher amount of these mineral phases, while for sample 2, a shoulder and not a sharp band can be observed, indicating lower contents of these phases when comparing only these bands.

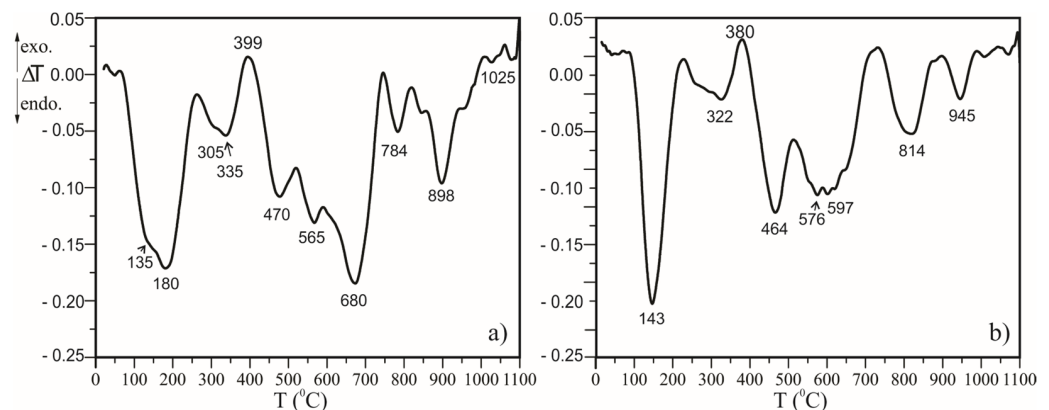


**Figure 6.** DTA data obtained for: (a) sample 1 and (b) sample 2.

An OH component is released from goethite mineral or other iron hydroxides at temperatures between 260 and 400 °C, where the conversion of  $\text{Fe}_2\text{O}_3$  into  $\text{Fe}_3\text{O}_4$  occurs after the process of hydroxylation [51–53]. The exothermic band around 400 °C indicates the presence of organic matter [51,54] in both of the investigated samples. The broad endothermic peak between 500 and 600 °C, observed in both samples, is the result of dehydroxylation of the octahedral sheet and can be related to different amounts of illite, chlorite, kaolinite, and smectite minerals [25,55]. The peak at 470 °C indicates the destruction of the crystal lattice of minerals from the phyllosilicate group, and it can be observed with a slightly higher intensity in sample 2 compared to sample 1. Chlorites exhibit a thermal curve appearing as a broad and intense endothermic peak at temperatures between 550 and 670 °C paired with a smaller, sometimes hardly visible, narrow exothermic peaks at temperatures between 805 and 875 °C [51]. The bands that correspond to chlorite minerals, around 597 °C for sample 2 and 680 °C for sample 1, are of different intensities, indicating a higher content of this phase in sample 1. This is in good agreement with the XRD data obtained for the investigated samples. The bands between 800 and 850 °C, present as large endothermic bands, indicate the presence of carbonate minerals. The presence of well-expressed double thermal effects of carbonate thermal decomposition in sample 1 indicates a slightly higher content of these minerals when compared to sample 2. The exothermic reaction observed at around 950 °C corresponds to smectite minerals, such as montmorillonite [51,56–58]. Additionally, there was a smaller amount of minerals from the kaolinite group compared to other clay minerals. The absence of a characteristic peak that describes the transition of meta-kaolinite to mullite indicates that both of the samples contained a smaller amount of minerals from the kaolinite group. Sample 1 had higher contents of illite, chlorite, and carbonate minerals compared to sample 2, giving it a slightly different thermal reaction.

The results of the infrared spectroscopy investigation for samples 1 and 2 are shown in Figure 7. Upon comparison with the literature data, it was determined that the sample was composed of a complex mixture of various minerals, including those from the clay group

(illite, smectite, kaolinite), feldspar, carbonate, iron hydroxide/oxide, and quartz [59–62], in addition to organic matter. The identification process was complicated due to the overlapping characteristic peaks of several different minerals, owing to the sample's polymineral composition. The peaks at 470, 525, 648, 915, and 3450  $\text{cm}^{-1}$ , as well as the peak at 915  $\text{cm}^{-1}$ , indicate the presence of minerals from the smectite–illite groups of clays [59]. The presence of hydromica and illite is additionally confirmed by the appearance of peaks at 3599 and 999  $\text{cm}^{-1}$ . Minerals from the kaolinite group are indicated by the smaller peaks at 3460, 1629, 945, 912, 470, and 430  $\text{cm}^{-1}$  [59–61], although these peaks are of a smaller intensity and can overlap with minerals from the mica group. The peaks at 470, 525, 690, 780, 800, 1090, and 1152  $\text{cm}^{-1}$  correspond to quartz, while the peaks at 430, 470, 525, 648, 730, 780, 1005, 1090, and 1160  $\text{cm}^{-1}$  correspond to feldspars [62].

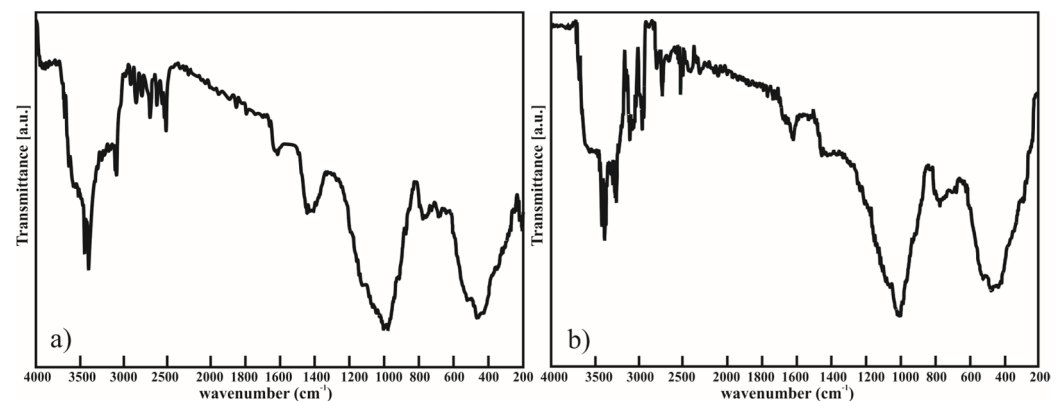


**Figure 7.** The results of the infrared spectroscopy investigation for: (a) sample 1 and (b) sample 2.

The presence of carbonate is indicated by the peaks at 1445, 875, and 730  $\text{cm}^{-1}$ . The carbonate peaks are of higher intensity for sample 1 compared to sample 2, indicating a slight difference in the carbonate content. Ferrous minerals were identified by peaks at 410, 470, 680, 800, 1038, 1090, and 1660  $\text{cm}^{-1}$  [62]. The hydroxyl group was observed by the presence of peaks at 3610 and 3370  $\text{cm}^{-1}$ , while the peak at 1629  $\text{cm}^{-1}$  corresponded to the presence of water in the sample [63]. Organic matter was observed at wavelengths of 980, 1152, 1408, 1629, 2860, 2925, 2510, 2610, 2700, 2795, 3405, and 3645  $\text{cm}^{-1}$ , indicating vibrations of  $\text{CH}_2$ ,  $\text{COOH}$ , and humin [64,65]. Sample 2 was similar to sample 1 and contained a mixture of minerals, such as clay, feldspar, carbonate, iron oxide or hydroxide, and quartz. However, sample 1 had a higher content of carbonaceous minerals when compared to sample 2. This is indicated by the higher intensity of the band around 1445  $\text{cm}^{-1}$ . This statement is supported by the chemical analysis of both samples, as shown in Table 2. The intensity of the bands corresponding to the hydroxyl group and water is slightly higher for sample 1 compared to sample 2. This indicates that the water content in the former was different from the latter. The most noticeable difference between the two samples is the band around 1400  $\text{cm}^{-1}$  which has significantly higher intensity in sample 1. This difference is also reflected in the percentage of the mass lost during ignition, as shown in Table 2, where we can observe slight differences between the samples.

The results of the chemical analyses of both of the investigated samples are presented in Table 2. Samples 1 and 2 contained high levels of silica (>52 wt.%) and alumina (~16 wt.%), with around 6 wt.%  $\text{Fe}_2\text{O}_3$ , 2.8 wt.%  $\text{K}_2\text{O}$ , 4.8 wt.%  $\text{CaO}$ , and 2.9 wt.%  $\text{MgO}$  as the main constituents. The mass ratio of  $\text{SiO}_2/\text{Al}_2\text{O}_3$  ranged from 3.45 to 3.62 for samples 1 and 2, which was significantly higher than the values generally found for pure kaolinite (1.18), montmorillonite, or illite (2.36) [25] and is in good accordance with the XRD and DTA data, indicating the complex mixture of these minerals. These  $\text{SiO}_2/\text{Al}_2\text{O}_3$  ratios are probably due to abundant quartz and variable mineral contents of smectite/illite/chlorite in the samples studied [6,66–68].

**Table 2.** Chemical analysis of the investigated samples.

Oxides (wt.%)	Sample 1	Sample 2
SiO <sub>2</sub>	52.8	58.3
Al <sub>2</sub> O <sub>3</sub>	15.3	16.1
Fe <sub>2</sub> O <sub>3</sub>	6.9	6.8
MnO	0.1	0.1
MgO	2.9	2.2
CaO	4.8	1.2
Na <sub>2</sub> O	1.5	1.5
K <sub>2</sub> O	2.9	2.9
TiO <sub>2</sub>	0.8	0.9
P <sub>2</sub> O <sub>5</sub>	0.2	0.2
SO <sub>3</sub>	u.d.	u.d.
LOI	12.5	10.4
Sum	100.7	100.6

Note: u.d.—under the detection limits.

Sample 1 had a higher content of CaO, with 4.8%, in comparison to the 1.2% observed in sample 2. Higher contents of Ca oxides and Mg oxides indicate the presence of carbonate and/or chlorite minerals [25], although this can be also attributed to the lower content of smectites that were observed in the XRD investigation of the samples. High mass loss on ignition (LOI) observed in both investigated samples may be associated with the higher contents of clay minerals, such as illite and kaolinite, closely mixed with secondary minerals, such as carbonates, organic matter, and hydroxides [19,25], which were confirmed by differential thermal analysis and XRD investigations. Therefore, both of the samples can be regarded as silica-rich materials, making them beneficial for ceramic products. The contents of alkaline oxides (K<sub>2</sub>O and Na<sub>2</sub>O), probably originating from feldspars and clay minerals, could further indicate the presence of the natural contents of flux materials. Upon analyzing the trace amounts of elements found in the investigated samples, it was discovered that barium (Ba), chromium (Cr), rubidium (Rb), strontium (Sr), vanadium (V), and yttrium (Y) were present in abundance, with over 100 ppm per sample (Table 3). The other tested elements had lower contents than these.

**Table 3.** The trace amounts of elements found in the investigated samples.

Elements (ppm)	Sample 1	Sample 2
Ba	674	635
Ce	88	89
Co	25	22
Cr	118	122
Cs	8	6
Cu	45	44
Ga	18	20
Gd	9	11
La	42	45
Nb	14	15
Nd	37	38

Table 3. Cont.

Elements (ppm)	Sample 1	Sample 2
Ni	55	53
Pb	27	28
Pb	27	28
Pr	10	11
Rb	115	126
Sc	19	21
Sm	9	11
Sr	198	139
Th	14	14
U	1	u.d.
V	143	134
W	7	8
Y	31	34

Note: u.d.—under the detection limits.

Slightly soluble and extremely soluble salts and sulfates will cause efflorescence on the surface [69] of the product, while higher contents of elements such as Sr, Co, Cu, V, Fe, and Mn can lead to a color change during the firing of clay [70]. It has been reported that vanadium stains are most obvious on cream-colored bricks and are usually green or yellow [71]. They form in the clay during firing processes and are transported as soluble potassium and sodium compounds to the brick surface, where the oxidation of vanadium compounds occurs [71]. Although efflorescence is not harmful to the user of the pottery, some reported efflorescence tests showed that the addition of magnesite (1 wt.%) removed the incidence of vanadium staining, while calcite and fluorspar additions were not as effective [71]. By adding barium compounds, such as barium carbonate, barium chloride, or barium hydroxide to the raw material, the soluble sulfate salts were converted into insoluble barium sulfate, reducing the effect of efflorescence, while with the addition of 2.0 wt.% barium carbonate, no efflorescence was observed [72]. Slightly higher contents of elements such as Ba and Mg in the investigated samples could contribute to the lower formation of salts that lead to the production of efflorescence in the final product.

The cation exchange capacity (CEC) is a measure of the quantity of exchanged cations and is crucial in evaluating the quality of clays. Different types of clay minerals can be classified as inert, including chlorite, illite, and kaolinite, which have a cationic exchange capacity ranging from 3 to 25 meq/100 g and a specific surface area of 10 to 100 m<sup>2</sup>/100 g [73]. Samples 1 and 2 demonstrated CEC values of 12.48 and 13.74 meq/100 g and specific surface area (SSA) values of 97.73 and 107.58 m<sup>2</sup>/100 g, respectively. Therefore, the samples can be described as mostly illite clay with a significant amount of chlorite type of minerals. The literature data indicate that ball and marly clays are known for having a wide methylene blue index range from 8 to 40 meq/100 g [74]. This allows for classifying these types of clays, based on their theoretical technological performance, as high-plasticity clays with a methylene blue index between 12 and 16.

The color of raw clay can be influenced by various factors, such as mineralogical and chemical composition, geological locality, how deeply it was mined, and the influence of atmospheric forces. The color of raw clay that is mined from shallow deposits may be affected by the presence of organic matter covering it on the surface. Additionally, heavy precipitation and subsequent flooding can introduce other substances that may also impact the color of the clay. The Munsell cards for the dry samples 1 and 2 show a yellowish brown (10YR5/4) and brown (5YR4/4) color, respectively. The color saturation differed between sample 1 and sample 2 since they had a large difference in their contents

of CaO (4.8 and 1.2 wt.%) and slight differences in their contents of MnO (0.1 and 0.1 wt.%) and TiO<sub>2</sub> (0.8 and 0.9 wt.%), respectively. The creamy yellowish brown color observed in sample 1 could be attributed to the combination of Ca with other elements, like Sr and Mn, and Ti minerals, such as rutile [75]. The presence of Cr is likely to result in darker yellow shades [76], although the content of this element in both samples was similar. The investigated samples had a higher content of naturally present Fe oxides, above 6 wt.%. Fe<sup>3+</sup> is responsible for the brown, yellow, black, and red colors after firing [77], and its concentration also matters—less than 1 wt.% Fe (as oxide) produces a white color, 1–2 wt.% imparts a yellow color, 2–3 wt.% produces a smooth color, and 4–5 wt.% and above give red hues [75]. The combination of higher Fe<sub>2</sub>O<sub>3</sub> and lower CaO present in sample 2 alongside other elements yielded a darker shade of brown. The color can also be affected by the presence of organic matter. Clays with an Fe<sub>2</sub>O<sub>3</sub> content higher than 5% could be described as “dark-firing” ceramic bodies, while those with an Fe<sub>2</sub>O<sub>3</sub> content less than 5% could be classified as “light-firing” ceramic bodies [5,43,78]. It is worth noting that compared to other oxides, the Fe<sub>2</sub>O<sub>3</sub> content was highest in the samples. Based on this factor alone, the final color of the pottery product would be classified as a dark-firing body, which would presumably fire in dark red hues.

## 5. Conclusions

The raw clay samples from the Ražanj deposit in Serbia consisted mainly of clay types of minerals, illite, smectite, and chlorite. The secondary minerals that comprised the clays were quartz, feldspars, Fe minerals (goethite and limonite), and carbonate minerals, present in different amounts in the investigated samples. Sample 1 exhibited a slightly higher abundance of illite, smectite, and chlorite minerals with a lower quartz content compared to sample 2. All applied investigative methods confirmed the mineralogical composition of the samples. Chemical analysis showed a relatively high abundance of silica and alumina with a mass ratio of SiO<sub>2</sub>/Al<sub>2</sub>O<sub>3</sub> that ranged from 3.45 (sample 1) to 3.62 wt.% (sample 2), and the higher amounts of SiO<sub>2</sub> correspond to the contents of quartz and feldspars in the investigated samples. The content of Fe<sub>2</sub>O<sub>3</sub> was similar in both investigated samples and was around 6 wt.%. Sample 1 had a slightly higher content of CaO (4.8 wt.%) compared with the 1.1 wt.% observed in sample 2. The contents of the trace elements in the investigated samples showed that barium (Ba), chromium (Cr), rubidium (Rb), strontium (Sr), vanadium (V), and yttrium (Y) were present in abundance, with over 100 ppm, with slight differences between the samples. According to the ternary diagram that represents the grain size, both samples can be described as loam, with roughly equal proportions of sand, silt, and clay, and moderately high porosity. The cation exchange capacity (CEC) measurements show that the samples varied between low- and middle-charged clay minerals (12.48 and 13.47 meq/100 g for samples 1 and 2, respectively), while the specific surface area (SSA) ranged from 97.73 to 107.58 m<sup>2</sup> × g<sup>−1</sup>, for samples 1 and 2, respectively. Visual inspection of the dry samples showed that sample 1 corresponded closely to a moderate yellowish brown (10YR5/4), while sample 2 was moderate brown (5YR4/4) in color.

Our findings indicate that, based on their mineralogical characteristics, the investigated raw clay samples from Ražanj are marly loam clays (illite–chlorite clay with smectite and carbonates and a higher content of quartz) with a higher iron content that would fire red (“dark-firing” ceramic bodies), and they are most suitable for application in the manufacture of traditional pottery. To better characterize the Ražanj deposit and its application in the ceramic industry, it is necessary to focus on further investigation, additional fieldwork, and other methods, as well as the technological characterization of the clays from this region.

**Author Contributions:** Conceptualization, methodology, writing—original draft preparation, M.M. and P.D.; software, writing—review and editing, M.R.; validation, writing—review and editing, V.D.; formal analysis, writing—review and editing, J.G. All authors have read and agreed to the published version of the manuscript.

**Funding:** This research was funded by the Ministry of Science, Technological Development and Innovation of Serbia, based on Contract no. 451-03-65/2024-03/200126 (Faculty of Mining and Geology); 451-03-66/2024-03/200126 (Faculty of Mining and Geology); 451-03-66/2024-03/200017 (“Vinča” Institute of Nuclear Sciences—National Institute of the Republic of Serbia).

**Data Availability Statement:** The data are contained within the article.

**Conflicts of Interest:** The authors declare no conflicts of interest. The funders had no role in the design of the study; in the collection, analyses, or interpretation of data; in the writing of the manuscript; or in the decision to publish the results.

## References

1. Norton, F.H. *Fine Ceramics Technology and Applications*; McGraw-Hill Book Company: New York, NY, USA, 1970; p. 507.
2. Burst, J.F. The application of clay minerals in ceramics. *Appl. Clay Sci.* **1991**, *5*, 421–443. [[CrossRef](#)]
3. Vieira, C.M.F.; Sánchez, R.; Monteiro, S.N. Characteristics of clays and properties of building ceramics in the state of Rio de Janeiro, Brazil. *Constr. Build. Mater.* **2008**, *22*, 781–787. [[CrossRef](#)]
4. Kamseu, E.; Leonelli, C.; Boccaccini, D.N.; Veronesi, P.; Miselli, P.; Pellacani, G.; Melo, U.C. Characterisation of porcelain compositions using two china clays from Cameroon. *Ceram. Int.* **2007**, *33*, 851–857. [[CrossRef](#)]
5. Milošević, M.; Logar, M. Properties and characterization of a clay raw material from Miličinica (Serbia) for use in the ceramic industry. *Clay Miner.* **2017**, *52*, 329–340. [[CrossRef](#)]
6. Milošević, M.; Dabić, P.; Kovač, S.; Kaluđerović, L.; Logar, M. Mineralogical study of clays from Dobrodo, Serbia, for use in ceramics. *Clay Miner.* **2019**, *54*, 369–377. [[CrossRef](#)]
7. Milošević, M.; Djordjević, B.; Zdravković, A. Structural characterization of traditional pottery produced from local clay, Rujšite (Ražanj, Central Serbia), to preserve its geoheritage. In Proceedings of the 9th International Conference Mineralogy and Museums, Sofia, Bulgaria, 24–26 August 2021; Extended Abstracts; pp. 92–93.
8. Bundy, W.M.; Ishley, J.N. Kaolin in paper filling and coating. *Appl. Clay Sci.* **1991**, *5*, 397–420. [[CrossRef](#)]
9. Murray, H.H. Overview—Clay mineral applications. *Appl. Clay Sci.* **1991**, *5*, 379–395. [[CrossRef](#)]
10. Minato, H.; Shibue, Y. A case for utilization of clays to raw materials of outside wall at final disposal site of town waste matters and new treatment techniques for polluted soils. *J. Clay Sci. Soc. Jpn.* **1999**, *38*, 167–180. [[CrossRef](#)]
11. Murray, H.H.; Kogel, J.E. Engineered clay products for the paper industry. *Appl. Clay Sci.* **2005**, *29*, 199–206. [[CrossRef](#)]
12. Viseras, C.; Aguzzi, C.; Cerezo, P.; Lopez-Galindo, A. Uses of clay minerals in semisolid health care and therapeutic products. *Appl. Clay Sci.* **2007**, *36*, 37–50. [[CrossRef](#)]
13. Silva-Valenzuela, M.G.; Matos, C.M.; Shah, L.A.; Carvalho, F.M.S.; Sayeg, I.J.; Valenzuela-Diaz, F.R. Engineering Properties of Kaolinitic Clay with Potential Use in Drugs and Cosmetics. *Int. J. Mod. Eng. Res.* **2013**, *3*, 163–165.
14. Valášková, M. Clays, clay minerals and cordierite ceramics—A review. *Ceram.-Silikáty* **2015**, *59*, 331–340.
15. Carretero, M.I.; Pozo, M. Clay and Non-Clay Minerals in the Pharmaceutical Industry: Part I. Excipients and Medical Applications. *Appl. Clay Sci.* **2009**, *46*, 73–80. [[CrossRef](#)]
16. Meunier, A. *Clays*, 1st ed.; Springer: Berlin/Heidelberg, Germany, 2005; p. 472. [[CrossRef](#)]
17. Murray, H.H. Applied clay mineralogy today and tomorrow. *Clay Miner.* **1999**, *34*, 39–49. [[CrossRef](#)]
18. Chang, L.L.Y. *Industrial Mineralogy: Materials, Processes, and Uses*, 1st ed.; Prentice Hall: Upper Saddle River, NJ, USA, 2002; p. 472.
19. Schroeder, P.A.; Erickson, G. Kaolin: From ancient porcelains to nanocomposites. *Elements* **2014**, *10*, 177–182. [[CrossRef](#)]
20. Mukherjee, S. *The Science of Clays—Applications in Industry, Engineering and Environment*, 1st ed.; Springer: Dordrecht, The Netherlands; Capital Publishing Company: New Delhi, India, 2013; p. 335. [[CrossRef](#)]
21. Dondi, M. Technological and compositional requirements of clay materials for ceramic tiles. In Proceedings of the 12th International Clay Conference, Bahía Blanca, Argentina, 22–28 July 2001; Domínguez, E.A., Mas, G.R., Cravero, F., Eds.; Elsevier: Amsterdam, The Netherlands, 2003; pp. 23–30. [[CrossRef](#)]
22. Grimshaw, R.W. *The Chemistry and Physics of Clays and Allied Ceramic Materials*, 4th ed.; Ernest Benn Limited: London, UK, 1971; p. 1024.
23. Saikia, N.J.; Bharali, D.J.; Sengupta, P.; Bordoloi, D.; Goswamee, R.L.; Saikia, P.C.; Borthakur, P.C. Characterization, beneficiation and utilization of a kaolinite clay from Assam, India. *Appl. Clay Sci.* **2003**, *24*, 93–103. [[CrossRef](#)]
24. Mitrović, A.A.; Komljenović, M.M.; Ilić, B.R. Ispitivanja mogućnosti korišćenja domaćih kaolinskih glina za proizvodnju metakaolina. *Hem. Ind.* **2009**, *63*, 107–113. [[CrossRef](#)]
25. Boussem, S.; Sghaier, D.; Chaabani, F.; Jamoussi, B.; Bennour, A. Characteristics and industrial application of the Lower Cretaceous clay deposits (Bouhedma Formation), Southeast Tunisia: Potential use for the manufacturing of ceramic tiles and bricks. *Appl. Clay Sci.* **2016**, *123*, 210–221. [[CrossRef](#)]
26. Vandiver, P.B.; Soffer, O.; Klima, B.; Svoboda, J. The Origins of Ceramic Technology at Dolni Vestonice, Czechoslovakia. *Science* **1989**, *246*, 1002–1008. [[CrossRef](#)]
27. Milošević, M.; Logar, M.; Djordjević, B. Mineralogical analysis of a clay body from Zlakusa, Serbia, used in the manufacture of traditional pottery. *Clay Miner.* **2020**, *55*, 142–149. [[CrossRef](#)]

28. Rye, O.S. *Pottery Technology; Principles and Reconstructions*; Manuals on Archaeology No. 4; Taraxacum: Washington, DC, USA, 1981.
29. Rice, P.M. *Pottery Analysis: A Sourcebook*; University of Chicago Press: Chicago, IL, USA, 1987.
30. Roux, V. *Ceramics and Society: A Technological Approach to Archaeological Assemblages*; Springer Nature: Cham, Switzerland, 2019; p. 329.
31. Ho, J.W.I.; Quinn, P.S. Intentional clay-mixing in the production of traditional and ancient ceramics and its identification in thin section. *J. Archaeol. Sci. Rep.* **2021**, *37*, 102945. [\[CrossRef\]](#)
32. Müller, N.S. Mechanical and thermal properties. In *The Oxford Handbook of Archaeological Ceramic Analysis*; Hunt, A., Ed.; Oxford University Press: Oxford, UK, 2016; pp. 321–342.
33. Vasić, M.V.; Pezo, L.L.; Zdravković, J.D.; Vrebalov, M.; Radojević, Z. Thermal, ceramic and technological properties of clays used in the production of roofing tiles—Principal component analysis. *Sci. Sinter.* **2018**, *50*, 487–500. [\[CrossRef\]](#)
34. Vasić, M.R.; Vasić, M.V. Optimize, upgrade or invest in a novel dryer?—A brick factory case study. *Int. J. Manuf. Econ. Manag.* **2021**, *2*, 62–70. [\[CrossRef\]](#)
35. Available online: <https://nkns.rs/cyr/novi-upisi-u-nacionalni-registar-nematerijalnog-kulturnog-nasledja-0> (accessed on 4 April 2024).
36. Đorđević, B. *Ražanjско Crepuljarstvo—Izrada Crepulja u Rujištu kod Ražnja*; Turistička Organizacija Ražanj i Etnografski Muzej u Beogradu: Čigoja, Beograd, 2021; p. 100.
37. Savić, M.M. Kućna industrija u Srbiji pre 1912. god., Naša industrija, zanati i trgovina, njine osnovice, stanje, odnosi, važnost, putevi, prošlost i budućnost. *Sarajevo* **1928**, *6*, 264–271.
38. Krstić, B.; Veselinović, M.; Divljan, M.; Rakić, M. *Osnovna Geološka Karta 1:100,000*; Tumač za list Aleksinac K 34-20; Savezni geološki: Zavod, Beograd, 1980; p. 59.
39. Milošević, M. Mineralogy of clay used for pottery manufacture in Rujište (Ražanj, Serbia). In Proceedings of the 18th Serbian Geological Congress “Geology Solves the Problems”, Divčibare, Serbia, 1–4 June 2022; p. 175.
40. *Rigaku PDXL 2: Integrated Powder X-ray Diffraction Software*; Version 2.8.4.0; Rigaku Corporation: Tokyo, Japan, 2007.
41. Gates-Rector, S.; Blanton, T. The powder diffraction file: A quality materials characterization database. *Powder Diffr.* **2019**, *34*, 352–360. [\[CrossRef\]](#)
42. ASTM Standard test method for methylene blue index of clay (C 837-99). In *1984 Annual Book of ASTM Standards, Sect. 15, Vol. 15.02*; American Society for Testing and Materials (ASTM): Philadelphia, PA, USA, 1984.
43. Abadir, M.F.; Sallam, E.H.; Bakr, I.M. Preparation of porcelain tiles from Egyptian raw materials. *Ceram. Int.* **2002**, *28*, 303–310. [\[CrossRef\]](#)
44. Jackson, G. *Introduction to Whiteware*; Elsevier Publishing Company: Amsterdam, The Netherlands, 1969; p. 147.
45. Rivi, A.; Ries, B. Single-line dry grinding technology. *Ceram. World* **1997**, *24*, 132–141.
46. McManus, J. Grain size distribution and interpretation. In *Techniques in Sedimentology*; Tucker, M.E., Ed.; Blackwell: Oxford, UK, 1988; pp. 63–85.
47. Strazzera, B.; Dondi, M.; Marsigli, M. Composition and ceramic properties of Tertiary clays from Southern Sardinia (Italy). *Appl. Clay Sci.* **1997**, *12*, 247–266. [\[CrossRef\]](#)
48. El Ouahabi, M.; Daoudi, L.; Fagel, N. Mineralogical and geotechnical characterization of clays from northern Morocco for their potential use in the ceramic industry. *Clay Miner.* **2014**, *49*, 35–51. [\[CrossRef\]](#)
49. Bradley, W.F.; Grim, R.E. High temperature thermal effects of clay and related materials. *Am. Mineral.* **1951**, *36*, 182–201.
50. Grim, R.E.; Rowland, R.A. Differential thermal analysis of clays and shales, control and prospecting method. *J. Am. Ceram. Soc.* **1944**, *27*, 65–76. [\[CrossRef\]](#)
51. Földvári, M. Handbook of thermogravimetric system of minerals and its use in geological practice. In *Occasional Papers of the Geological Institute of Hungary*; Maros, G., Ed.; Geological Institute of Hungary: Budapest, Hungary, 2011; Volume 213, p. 180.
52. Sinuhaji, M.M.F.; Harjanto, S.; Hapid, A. Thermal characteristics and phase transformation of iron ores containing varied crystalline water with coal mixtures. Conference on Innovation in Technology and Engineering Science. *IOP Conf. Ser. Mater. Sci. Eng.* **2019**, *602*, 012065. [\[CrossRef\]](#)
53. Babich, A.; Senk, D.; Gudenau, H.W.; Mavrommatis, K. *Ironmaking*; Verlagshaus Mainz GmbH: Aachen, Germany, 2008; p. 402.
54. Yariv, S. Differential Thermal Analysis (DTA) in the Study of Thermal Reactions of Organo-Clay Complexes. In *Natural and Laboratory-Simulated Thermal Geochemical Processes*; Ikan, R., Ed.; Springer: Dordrecht, The Netherlands, 2003; pp. 253–296. [\[CrossRef\]](#)
55. Brown, G.; Brindley, G.W. *Crystal Structures of Clay Minerals and Their X-ray Identification*; Mineralogical Society: London, UK, 1984; p. 495.
56. Okada, K.; Otsuka, N. Characterization of spinel phase from SiO<sub>2</sub>–Al<sub>2</sub>O<sub>3</sub> xerogels and the formation process of mullite. *J. Am. Cer. Soc.* **1986**, *69*, 652–656. [\[CrossRef\]](#)
57. Gonzalez-Garcia, F.; Romero-Acosta, V.; Garcia-Ramos, G.; Gonzalez-Rodriguez, M. Firing transformations of mixtures of clays containing illite, kaolinite and calcium carbonate used by ornamental tile industries. *App. Clay Sci.* **1990**, *5*, 361–375. [\[CrossRef\]](#)
58. Aras, A. The change of phase composition in kaolinite- and illite-rich clay-based ceramic bodies. *App. Clay Sci.* **2004**, *24*, 257–269. [\[CrossRef\]](#)
59. Madejová, J. FTIR techniques in clay mineral studies. Review. *Vib. Spectrosc.* **2003**, *31*, 1–10. [\[CrossRef\]](#)

60. Madejová, J.; Kečkéš, J.; Pálková, H.; Komadel, P. Identification of components in smectite/kaolinite mixtures. *Clay Miner.* **2002**, *37*, 377–388. [[CrossRef](#)]
61. de Almeida Azzi, A.; Osacký, M.; Uhlík, P.; Čaplovičová, M.; Zanardo, A.; Madejová, J. Characterization of clays from the Corumbataí formation used as raw material for ceramic industry in the Santa Gertrudes district, São Paulo, Brazil. *App. Clay Sci.* **2016**, *132–133*, 232–242. [[CrossRef](#)]
62. Chukanov, N. *Infrared Spectra of Mineral Species. Extended Library*; Springer: Dordrecht, The Netherlands; Heidelberg, Germany; New York, NY, USA; London, UK, 2014; Volume 1, p. 1726. [[CrossRef](#)]
63. Chukanov, N.; Chervonnyi, A. *Infrared Spectroscopy of Minerals and Related Compounds*; Springer International Publishing: Geneva, Switzerland, 2016; p. 1109. [[CrossRef](#)]
64. Helal, A.A.; Murad, G.A.; Helal, A.A. Characterization of different humic materials by various analytical techniques. *Arab. J. Chem.* **2011**, *4*, 51–54. [[CrossRef](#)]
65. Nuzzo, A.; Buurman, P.; Cozzolino, V.; Spaccini, R.; Piccolo, A. Infrared spectra of soil organic matter under a primary vegetation sequence. *Chem. Biol. Technol. Agric.* **2020**, *7*, 6. [[CrossRef](#)]
66. Soleimani, M.A.; Naghizadeh, R.; Mirhabibi, A.R.; Golestanifard, F. Effect of Calcination Temperature of the Kaolin and Molar Na<sub>2</sub>O/SiO<sub>2</sub> Activator Ratio on Physical and Microstructural Properties of Metakaolin Based Geopolymers. *Iran. J. Mater. Sci. Eng.* **2012**, *9*, 43–51.
67. Prud'homme, E.; Autef, A.; Essaidi, N.; Michaud, P.; Samet, B.; Joussein, E.; Rossignol, S. Defining Existence Domains in Geopolymers through Their Physicochemical Properties. *Appl. Clay Sci.* **2013**, *73*, 26–34. [[CrossRef](#)]
68. Mawoulikplim Anove, K.; Tchegueni, S.; Agbegnigan Degbe, K.; Fiatty, K.; Koriko, M.; Drogui, P.; Tchchangbedji, G. Physico-Chemical and Mineralogical Characterizations of Two Togolese Clays for Geopolymer Synthesis. *J. Miner. Mater. Charact. Eng.* **2022**, *10*, 400–409. [[CrossRef](#)]
69. Brownell, W.E. Fundamental factors influencing efflorescence of clay products. *J. Am. Ceram. Soc.* **1949**; *32*, 375–389. [[CrossRef](#)]
70. Fromme, R. Basic Flux Oxides in Glazes: Tutorial IV (Ceramics Web) 1994. Available online: [https://ceramicsweb.org/articles/glaze\\_tech/basic\\_flux\\_oxides.html](https://ceramicsweb.org/articles/glaze_tech/basic_flux_oxides.html) (accessed on 2 April 2024).
71. Phillips, D.N. Vanadium staining in fired red clay bricks. *Br. Ceram. Trans.* **2003**, *102*, 257–260. [[CrossRef](#)]
72. Jindasuwan, S.; Chakornnipit, P.; Sitthisuntorn, S. Influences of Inhibitor and Firing Temperature of Efflorescence Reduction of Clay Products. *Key Eng. Mater.* **2015**, *659*, 111–115. [[CrossRef](#)]
73. Chiappone, A.; Marelllo, S.; Scavia, C.; Setti, M. Clay mineral characterization through the methylene blue test: Comparison with other experimental techniques and applications of the method. *Can. Geotech. J.* **2004**, *41*, 1168–1178. [[CrossRef](#)]
74. Dondi, M.; Raimondo, M.; Zanelli, C. Clays and bodies for ceramic tiles: Reappraisal and technological classification. *Appl. Clay Sci.* **2014**, *96*, 91–109. [[CrossRef](#)]
75. Wang, S.; Gainey, L.; Mackinnon, I.D.R.; Allen, C.; Gu, Y.; Xi, Y. Thermal behaviors of clay minerals as key components and additives for fired brick properties: A review. *J. Build. Eng.* **2023**, *66*, 105802. [[CrossRef](#)]
76. Charalambous, A.C.; Sakalis, A.J.; Kantiranis, N.A.; Papadopoulou, L.C.; Tsirliganis, N.C.; Stratis, J.A. Cypriot byzantine glazed pottery: A study of the Paphos workshops. *Archaeometry* **2010**, *52*, 628–643. [[CrossRef](#)]
77. Molera, J.; Vendrell-Saz, M.; Garcia-Valles, M.; Pradell, T. Technology and colour development of Hispano-Moresque lead-glazed pottery. *Archaeometry* **1997**, *39*, 23–39. [[CrossRef](#)]
78. Murray, H.H. Applied Clay Mineralogy. Occurrences, processing, and application of kaolins, bentonites, palygorskite, sepiolite, and common clays. In *Developments in Clay Science*, 1st ed.; Elsevier Science: Amsterdam, The Netherlands, 2007; Volume 2, 180p. [[CrossRef](#)]

**Disclaimer/Publisher's Note:** The statements, opinions and data contained in all publications are solely those of the individual author(s) and contributor(s) and not of MDPI and/or the editor(s). MDPI and/or the editor(s) disclaim responsibility for any injury to people or property resulting from any ideas, methods, instructions or products referred to in the content.